IEEE Access
Multidisciplinary : Rapid Review : Open Access Journal

Received 22 October 2025, accepted 13 November 2025, date of publication 17 November 2025, date of current version 25 November 2025.

Digital Object Identifier 10.1109/ACCESS.2025.3633571

APPLIED RESEARCH

Submerged Stadium-Shaped Pressure Differential Dielectric Elastomer Generator for Wave Energy Conversion

MARCO CASELLI[1], AMEDEO CARLONI[1], ANTONELLO CHERUBINI[2], GIACOMO MORETTI[2], MARCO FONTANA[3], AND ROCCO VERTECHY[1]
[1]Department of Industrial Engineering, University of Bologna, 40136 Bologna, Italy
[2]Department of Industrial Engineering, University of Trento, 38123 Trento, Italy
[3]Institute of Mechanical Intelligence, Scuola Superiore Sant'Anna, 56100 Pisa, Italy

Corresponding author: Rocco Vertechy (rocco.vertechy@unibo.it) and Marco Fontana (marco.fontana@santannapisa.it)

The work of Marco Fontana was supported by Italian Ministry of University and Research (MUR) through Next Generation EU, Mission 4 Component 1, Project: Zipping Electro-Active Polymers for High-Performance Miniature Actuators (ZEAP) under Grant CUP J53C24002700006. The work of Giacomo Moretti was supported by European Union through ERC Starting Grant Project flEAP under Grant GA: 101163668.

ABSTRACT Ocean wave energy is a promising renewable resource, but its exploitation is limited by the cost and complexity of conversion systems. Dielectric Elastomer Generators (DEGs) are emerging as lightweight, corrosion-resistant, and scalable alternatives. This paper introduces a Pressure Differential Wave Energy Converter based on a stadium-shaped submerged DEG (SS-PD-DEG). A finite element model was developed to describe the system electro elastic response, capturing the non-axisymmetric deformation of the membrane under uniform and hydrostatic loading and to predict capacitance variations. A small-scale prototype was designed, manufactured, and tested both in air and underwater. Results confirmed the capability of the SS-PD-DEG to perform full energy generation cycles while operating in underwater conditions. Besides the demonstration of operation, in-air and submerged tests have confirmed the quality of the modelling approach and theoretical predictions. Underwater tests also demonstrated a hydrostatic-induced negative stiffness effect, enabling extended deformability and potential for broadband frequency response.

INDEX TERMS Dielectric elastomer generator, DEG, wave energy converter, stadium-shaped, submerged.

I. INTRODUCTION

Ocean wave energy represents a promising renewable resource due to its high energy concentration and strong predictability [1], [2], [3]. Despite these advantages, the elevated costs of marine infrastructure and the engineering challenges of creating durable devices capable of withstanding harsh ocean conditions have hindered the economic viability of current wave energy converter (WEC) technologies. As a result, wave energy remains largely in the pre-commercial phase, with only a limited number of full-scale WECs having been developed and tested [4], [5]. A new category of electro-mechanical transducers, known as Dielectric Elastomer Generators (DEGs), is currently being explored as an alternative Power Take-Off (PTO) technology for Wave Energy Converters (WECs) [6], [7]. DEGs are solid-state soft capacitors that generate direct current electricity by exploiting deformation-induced capacitance changes [8]. These devices are free from sliding or rolling mechanical components, are composed of inexpensive, flexible materials resilient to harsh marine conditions where conventional steel-based electromagnetic generators often fail, and provide high energy and power density relative to their mass [9], [10]. Together, these features make DEGs a compelling candidate to replace traditional PTO systems in WECs. Previous studies have examined integrating DEGs into oscillating water column (OWC) designs through both theoretical and experimental approaches [11], [12], demonstrating promising potential for energy and power output.

The associate editor coordinating the review of this manuscript and approving it for publication was Tao Wang.

More recent research has explored the implementation of circular submerged pressure differential WEC designs, demonstrating in wave tank experiments that purposely introduced negative stiffness mechanisms can achieve a broad frequency response [6], [13]. However, those studies restricted themselves to experimental analyses without the application of electrical activation on the dielectric membranes, focusing on the study of the fluid structure interaction problem without providing a full validation of the practical energy conversion capabilities of devices with submerged DEGs [13]. Additionally, those studies considered circular geometry for the DEG membrane, which is suitable for demonstration but holds limited potential for scaling up the device, because of the limited manufacturability of a membrane with large (metre scale) size in both planar directions.

In this work, we present a novel design for a submerged pressure differential WEC that utilizes DEG based on a stadium-shaped membrane (Fig. 1 and 2). We describe its design, fabrication, and experimental testing in small-scale underwater trials with fully active power generation. We experimentally characterize and demonstrate the energy conversion capability of this new system under both dry and submerged conditions. Results obtained from small-scale laboratory tests are extrapolated to real scale, providing preliminary proofs of feasibility for a full-scale wave energy converter based on this architecture.

The paper is organized as follows. Section II introduces the concept of the Submerged Stadium-Shaped Pressure Differential Dielectric Elastomer Generator (SS-PD-DEG), outlining its working principle, expected advantages over more conventional technologies, and highlighting the key physical phenomena involved in its operation. Section III presents the electromechanical modelling and design framework, including: the constitutive model of the elastomeric material based on custom made characterization experiments, and the implementation of a finite element model able to predict the complex electromechanical response of the system in-air and submerged conditions. Section IV describes the realization of a small-scale prototype, detailing the design and manufacturing of the DEG, a dedicated vessel, and a custom electronics and control system developed to operate and monitor the device. Section V reports on the experimental activities, comprising validation of the finite element model through capacitance and pressure–deflection measurements, and demonstration of complete energy generation cycles in both in-air and submerged conditions. This section also includes a discussion on how the small-scale results can be extrapolated to full-scale estimations. Finally, Section VI summarizes the main findings and contributions of the work.

II. STADIUM-SHAPED PRESSURE DIFFERENTIAL DEG

The core component of the proposed stadium-shaped DEG is a stretchable composite membrane made of alternating layers of conductive and dielectric materials forming a capacitor. The membrane is fixed along the perimeter of a stadium-shaped frame, leaving the central area unconstrained. When a differential pressure is applied across the membrane, it deforms out of plane into a three-dimensional shape (see Fig. 1-Top), which increases its capacitance by enlarging the electrode area and reducing the dielectric thickness. This capacitance variation can be exploited in cyclic operation, enabling the conversion of part of the mechanical work provided by an external variable-pressure source into electrical energy through the well-known four-phase cycle illustrated in Fig. 2.

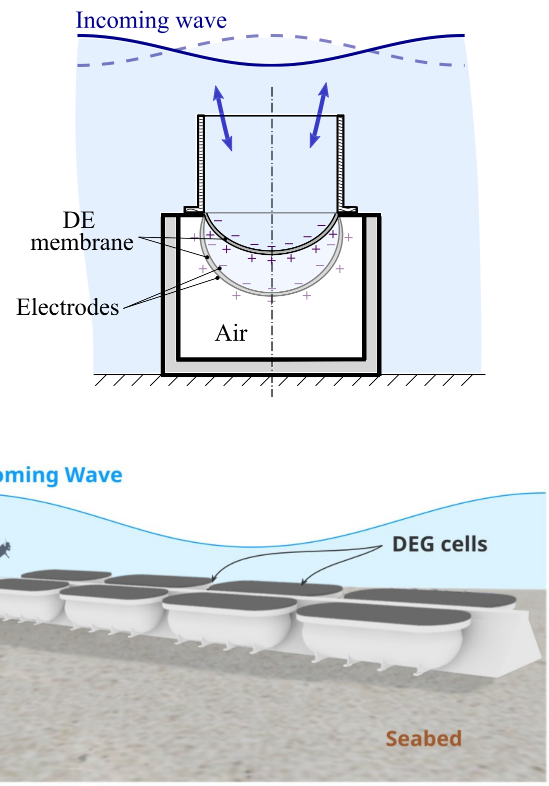

FIGURE 1. Concept of SS-PD-DEG. Top: representation of the operation, where wave induced pressure induces cyclic deformation of the DEG membrane. Bottom: artistic illustration of a possible full-scale concept for electricity generation from ocean waves, featuring an array of large-scale SS-PD-DEGs.

A stadium-shaped membrane is considered particularly attractive for the proposed wave-energy converter architecture because its elongated planform along one axis, while remaining compact along the other, confers two key advantages.

First, manufacturability: unlike large circular membranes—which, at the same active area, would require diameters of many meters and are impractical to produce with roll-to-roll equipment of limited lateral width—the stadium geometry attains the same area/capacitance target while keeping one side short, making it far more compatible with roll-to-roll film processing [14]. Although this may seem a minor technicality, it becomes a serious constraint at scale.

Second, hydrodynamic suitability: compared to the circular, axisymmetric layouts used in prior studies [13], for a given capacitance (and thus comparable power-conversion potential) the stadium aspect ratio allows the device length to be tuned relative to the wavelength without increasing the transverse span in the direction of wave propagation, thereby mitigating spatially non-uniform wave-pressure effects when device dimensions approach the wavelength.

Additionally, even if not demonstrated in this work, a submerged pressure-differential WEC based on a stadium-shaped DEG is expected to retain the key features observed with circular diaphragms—most notably the hydrostatic-induced negative-stiffness effect and, potentially, similar control strategies—thus potentially offering comparable broadband response with improved scalability.

Specifically, in this work, we propose integrating the stadium-shaped DEG into concepts of pressure differential WEC that have been explored by a few developers [15], [16]. These previous systems employ submerged air chambers enclosed in elongated vessels, with one large aperture sealed by a flexible passive membrane and another duct connecting the chamber to a pneumatic generator. The wave action drives the passive membrane, inducing volume and pressure variations that force airflow through the generator. Our concept replaces the passive membrane with an active one, implementing the Stadium-Shaped Pressure Differential DEG (SS-PD-DEG), thereby embedding the power take-off (PTO) directly into the membrane.

The SS-PD-DEG design thus offers multiple potential advantages over conventional pneumatic versions, including simpler installation and maintenance, lower capital and operating costs, intrinsic resistance to shock and corrosion, silent and vibration-free operation. At the same time, its operating principle introduces a rich and complex dynamic response, driven by the direct action of wave-induced pressure on the DEG membrane and by the inherently non-uniform, anisotropic out-of-plane deformation of the stadium-shaped geometry.

This complexity underscores the need for dedicated modelling and experimental validation. Key physical phenomena affecting the wave-membrane interaction process include:

- Air-chamber response: The periodic inward and outward motion of the membrane modulates the chamber volume, creating cyclical pressurization/depressurization cycles.
- Pre-pressurization of the vessel: Initial pre-pressurization of the chamber is necessary to maintain a flat membrane at rest, balancing hydrostatic pressure even in the absence of waves;
- Negative-stiffness effect: submerged pressure differential WECs display a hydrostatic-induced negative stiffness component—downward membrane deflection increases hydrostatic pressure, which further promotes deformation. This negative-stiffness effect can be leveraged to counterbalance, at least in part, the intrinsic elastic stiffness of the membrane and the air chamber, thereby allowing large deformations over a broad range of wave frequencies and amplitudes [6], [13], without the need for a resonant design.
- Direct water contact and voltage breakdown risk: since the SS-PD-DEG membrane operates in direct contact with seawater—a conductive environment—at high voltages (several kilovolts), there is a risk of charge leakage or dielectric breakdown. These issues are well-known in dielectric elastomer generator systems and must be carefully addressed for underwater operation.

To validate these dynamics and assess the energy conversion potential, this research work pursued the following steps:

- Design of a scaled prototype of the SS-PD-DEG cell to measure mechanical, electrical, and dynamic responses.
- Development and validation of a comprehensive FEM model incorporating purposely characterized material constitutive behavior.
- Construction of a dedicated experimental setup for the characterization of the SS-PD-DEG in air and submerged environments, and for the demonstration of its energy generation performance.
- Execution of quasi-static tests in both air and submerged conditions to experimentally demonstrate negative-stiffness effects and to compare underwater performance with operation in air.

The results of these activities are presented in the following sections.

III. MODELLING AND DESIGN

This section introduces a finite element (FE) modelling approach for the SS-PD-DEG, enabling the calculation of its deformed shape under different pressure boundary conditions (uniform and hydrostatic), together with the resulting strain distribution and electrical capacitance.

The complex geometry of the SS-PD-DEG, combined with the position-dependent pressure fields generated by hydrostatic loading, makes the system difficult to capture using lumped-parameter or analytical formulations. For this reason, a FE-based approach is adopted.

We first report the characterisation of the hyperelastic parameters of the reference dielectric elastomer material. These parameters are then incorporated into the FE model to predict the deformed geometry of the DEG and its capacitance variations.

The models presented here are used as reference tools for analysing the small-scale SS-PD-DEG systems developed in this work.

A. CHARACTERIZATION OF SS-PD-DEG MATERIALS

The SS-PD-DEG is made of elastomeric materials, whose elastic behaviour in the presence of large strains can be described through a hyperelastic model [17]. This section describes the characterization of the material that was used as a reference for this study. The DE material used in this work

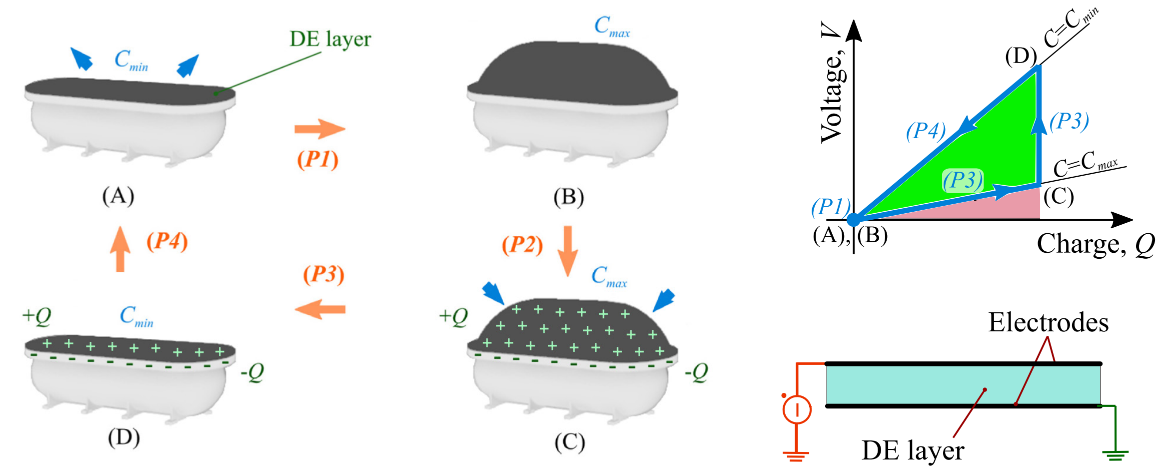

FIGURE 2. Working cycle of the stadium-shaped submerged dielectric elastomer generator at constant charge: graphical representation (left) and voltage-charge plot on the top right.

is the commercial silicone film ELASTOSIL 2030 by Wacker Chemie AG, with thickness of 200 μm. The stress-strain response of the film was measured through a test on a planar sample subject to pure shear deformations, with the setup of [18] shown in Fig. 3 - left. We used a sample with lateral width of 200 mm and longitudinal length (in the stretching direction) of 10 mm, so as to guarantee a deformation kinematics close to pure shear [19]. The lateral uniaxial prestretch is set to $\lambda_{2p} = 1.1$ which is close to the prestretch level which is chosen for the experimental prototype described in the following. The resulting nominal stress (per unit unstretched cross section area) is shown in Fig. 3-right.

Since the silicone dielectric elastomer exhibits only limited visco-plasticity once adequately pre-cycled (after approximately ten cycles) and can be accurately modeled as an incompressible solid, its mechanical response was analyzed by considering the average elastic behavior. Specifically, the average response was obtained as the mean between the loading and unloading curves over five consecutive cycles, and was then used to identify a suitable hyperelastic model consistent with the incompressibility condition. We used a Yeoh model for the fitting [20], which expresses the strain energy Ψ as a function of the principal stretches as follows:

$$\Psi_Y = \sum_{i=1}^{3} C_i \left(\lambda_1^2 + \lambda_2^2 + \lambda_1^{-2}\lambda_2^{-2} - 3\right)^i \tag{1}$$

where C_1, C_2 and C_3 are material constitutive parameters determined through numerical fitting of experimental data.

Fitting to the stabilized stress-strain response (tested up to $\lambda_{1,\max} = 3.4$) generates the following constitutive parameters: $C_1 = 169$ kPa, $C_2 = 0$, $C_3 = 577.4$ Pa for the Yeoh Model. The result of the fitting is reported in Fig. 3-bottom where the experimental data and the hyperelastic fitting are compared.

B. FE MODEL FORMULATION

The development of a simplified lumped model is often preferred over more complex numerical approaches such as finite-element (FE) modelling [6], [12]. However, for a stadium-shaped membrane the deformation field is non-uniform and non-axisymmetric, thus the description of its electromechanical response requires a use of FE tools. In this section, we describe the assumptions and implementative aspects of the FE analysis.

The constitutive material model defined in Section III-A was implemented in COMSOL Multiphysics and subsequently used to size the DEG membrane for the experimental tests reported in the following sections.

The SS-PD-DEG membrane is modelled using membrane elements, i.e., bending stiffness is neglected, no deformation gradient or stress are assumed to act in the thickness direction, and the undeformed membrane geometry is modelled as a 2D planar surface, lying on the xy axis of a reference frame (see Fig. 4). Owing to symmetries, only one quarter of the membrane is modelled. The membrane geometry in the unstretched configuration is obtained starting from a target final dimension of the holding frame, and scaling the dimensions in the two directions by their respective pre-stretches. Deformation of the membrane is applied as a two-step static study. In a first step, the membrane is provided with an in-plane pre-stretch through the application of prescribed displacements on the free portions of the perimeter. In a second step, the perimeter of the membrane is held fixed (i.e., a fixed displacement corresponding to pre-stretch provided in the first step), and a prescribed pressure is applied on one face of the membrane, pointing in the negative direction of the z axis. In the case of hydrostatic pressure acting on the membrane's face, the applied pressure is expressed as a function of the membrane's displacement, namely:

$$p = p_0 - \rho g w, \tag{2}$$

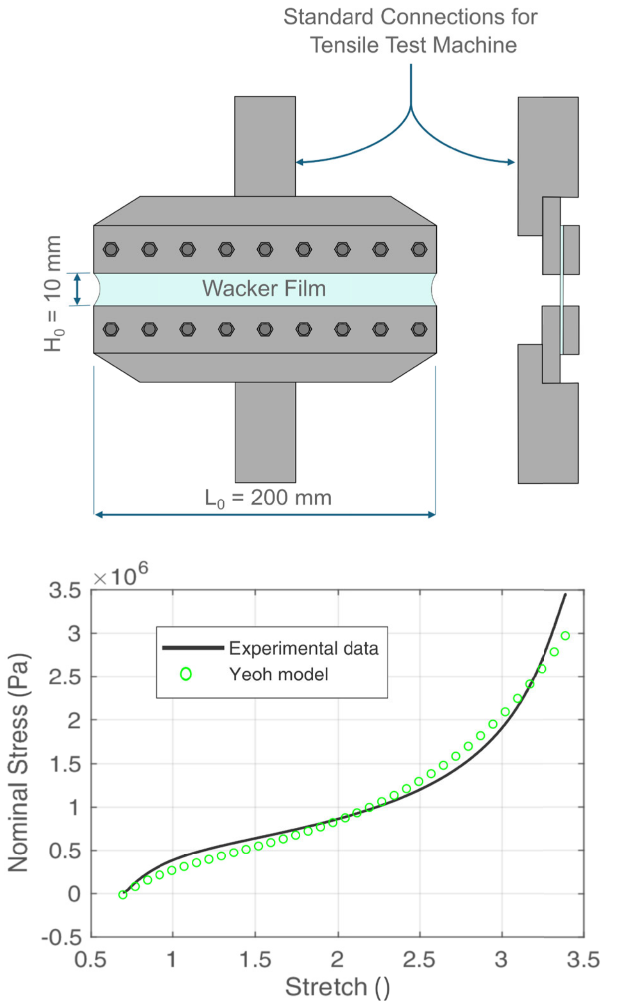

FIGURE 3. Characterization and fitting. Top:Drawing of the employed clamp for standard tensile testing machine employed for the characterization. Bottom: Experimental pure-shear stress-stretch response of the reference DE material (black) and hyperelastic fitting with the Yeoh model (green) (bottom).

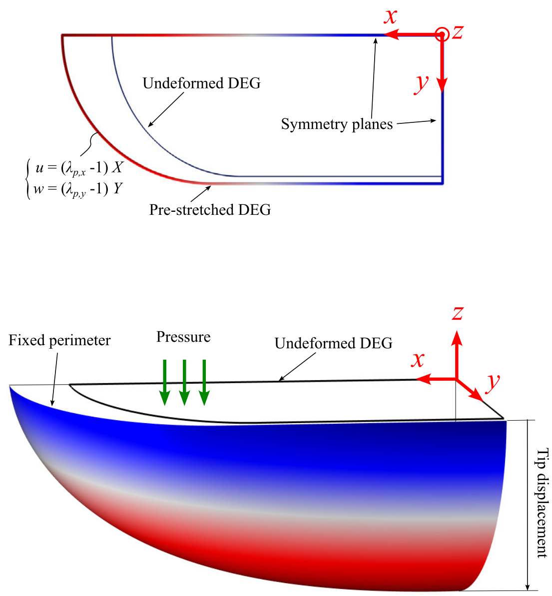

FIGURE 4. FE model implementation. Top: qualitative depiction of the DEG membrane's in-plane pre-stretching. The black line represents the unstretched membrane perimeter (one quarter of the whole geometry), whereas the colored line represents the perimeter after pre-stretch. Bottom: qualitative depiction of the DEG membrane deformation upon application of a pressure. In the plots, colours represent different displacement magnitudes.

where p_0 is an offset pressure, ρ is the water density, g is the acceleration of gravity, and w is a variable expressing the local displacement of a membrane's point in the z direction.

In the SS-PD-DEG application, in static conditions p_0 represents the difference between the hydrostatic pressure due to the water head h_w acting on the membrane perimeter, and the gauge air pressure p_a acting on the dry surface of the membrane: $p_0 = \rho g h_w - p_a$. In dynamic conditions in a wave energy application, the pressure p acting on the DEG (as given by Eq. (2)) should include additional contributions due to inertial/friction forces, the contribution of the radiated wave field, and the wave excitation pressure (which is in turn proportional to the wave height H), as detailed in [13]. The response to variable pressure differential is obtained by varying the offset pressure p_0, resulting in different deformed shapes.

The capacitance of the deformed membrane is obtained from the solution of the deformed shapes as:

$$C = \int_{A_0} \frac{\varepsilon \lambda_1 \lambda_2}{\lambda_3 t_d} dA_0, \tag{3}$$

where t_d is the undeformed thickness of the active dielectric layer (which differs from the total membrane thickness, as it does not include the contribution of the electrodes), ε is the dielectric permittivity, λ_1 and λ_2 are the principal stretches on the membrane surface, and λ_3 is the stretch in the thickness direction - constrained by the incompressibility relationship. The integral is calculated over the total unstretched surface A_0 of the DEG.

IV. SMALL-SCALE SS-PD-DEG PROTOTYPE AND TEST BENCH

A small-scale prototype of the proposed SS-PD-DEG has been designed, manufactured and tested, with the aim of: 1) validating the developed model presented in the previous section; 2) demonstrating the capability of the system to convert mechanical energy into electricity; 3) demonstrating the operation of the system when submerged in direct contact with water. The implemented prototype reflect the general architecture reported in Section I. The system includes the following main components:

1) Stadium shape DEG: membrane pre-stretched and fixed on a rigid frame that includes the electrical connections (more details on the manufacturing choices and process are provided in the following subsection).

2) The vessel: a rigid air-filled enclosure that presents on the top a stadium-shape aperture and a flange designed to host the DEG membrane as its cover. On the bottom two pneumatic connections allow the regulation of the internal pressure. The vessel is equipped with a laser distance sensor fixed on the bottom in order to be able to measure the out of plane displacement of the central point of the stadium shape (more details are provided in the following subsections).
3) Acquisition and driving electronics: an electronic system is employed to acquire the data from sensors during the tests and to drive high voltages during generation tests.

A scheme of the overall SS-PD-DEG small scale prototype is represented in Fig 6.

A. SS-PD-DEG MEMBRANE MANUFACTURING

The manufacturing process of the stadium-shaped membrane has been designed with the aim of obtaining a framed membrane that is ready to be used as the PTO element for the submerged DEG. In particular, the identified process includes the following four main phases: 1) pre-stretching, 2) framing and electrical connection preparation, 3) spray conductive coating for the electrodes on both sides of the membrane, and 4) spray coating of the water insulation layer on the external side of the membrane. Electrode and insulation deposition is purposely executed after pre-stretching in order to minimize the maximum stretch of these layers during operation.

As mentioned in the previous section, the employed dielectric film is the Wacker ELASTOSIL Film 2030 with a thickness of 200 μm, available in rolls several tens of meters long with a width of 200 mm. The geometric dimensions of the stadium-shaped membrane are chosen as $A = 436$ mm and $B = 170$ mm. This choice is mainly driven by two considerations: 1) the width $B = 170$ mm is the maximum allowed by the width of the commercial silicone elastomer film, considering that lateral margins are needed for pre-stretching and for fixation on the frame; 2) the length of $A = 436$ mm is chosen to obtain a stadium shape where the area of the rectangular central region is twice that of the two semicircular ends combined; this is to guarantee a clear distinction from a circular-shaped diaphragm.

The pre-stretches calculated in the previous section are applied starting from a sample of 600×200 mm of Wacker ELASTOSIL Film 2030 with a thickness of 200 μm. The membrane is first pre-stretched to $\lambda_1 = 1.15$ along the longer dimension with the help of two rigid bars. Then, the central part of the membrane, which is the part of the membrane that presents a uniform stretch, is laterally stretched up to $\lambda_2 = 1.05$ using two additional rigid bars (see Fig. 5). Once the membrane is stretched, one upper and one lower stadium-shaped frame are applied and connected. The frame keeps the membrane squeezed thanks to a crown of bolts that runs around the shape of the frame; additionally, a double-sided silicone adhesive is employed (NITTO P-905) between the frame and the membrane to prevent slipping. Copper tape is applied between the frames and the membrane in order to achieve the electrical connections. For the sake of reliability, two redundant electrical contacts are considered for each DEG electrode.

TABLE 1. DEG membrane capacitance and pressure summary.

DEG Membrane	Capacitance (nF) $h = 0$ mm	Capacitance (nF) $h = 87$ mm	Pressure (Pa) $h = 87$ mm
1	8.957	21.60	1250
2	8.94	20.25	1230
3	9.111	21.28	1290
4	8.83	20.29	1310
5	8.9	20.56	1340
6	8.64	19.58	1350
Average	8.90	20.59	1295
Std Dev	0.16	0.74	48.06

After the membrane is securely connected to the frames, the electrode deposition is performed through an airbrush. The sprayed mixture is composed of Orion PRINTEX®XE2 B BEADS carbon black (1.7% by weight), Wacker ELASTOSIL P 7670 silicone elastomer (24.6% by weight) and isopropyl alcohol (73.7% by weight), that first is mixed and degassed with a Thinky Mixer ARE-250CE. After each deposition, the membrane is cured in an oven. As a final step, an insulation coating is sprayed on the low-voltage side of the membrane — the one that comes into contact with water — using the same setup with a mixture of Wacker ELASTOSIL P 7670 and isopropyl alcohol and cured in an oven.

A total of six nominally identical stadium-shaped DEG membrane-frame assemblies have been manufactured and electrically tested. To assess repeatability, all the six manufactured DEG membranes have been tested to characterize their pressure and capacitance vs. tip displacement responses. A summary of the results is reported in Table 1, which highlight the consistency of the manual manufacturing process employed to realize the six DEG membranes (for both capacitance and inflation pressure measurements, the ratio between standard deviation and mean values is below 4%).

B. TEST BENCH DESIGN AND MANUFACTURING

The developed PTO membrane is hosted by a purposely designed vessel, as shown in Fig. 6. The vessel features a large flange on the top that allows for a watertight connection with the membrane frame. Sealing is obtained through a rubber gasket that has been laser-cut to match the shape and hole pattern of the flange. The vessel presents two small 1/8-inch apertures for pneumatic connection in order to regulate the internal pressure. Specifically, an external compressor is employed to provide pressurization, and a regulated leak valve is used to accurately tune the pressure and to rapidly

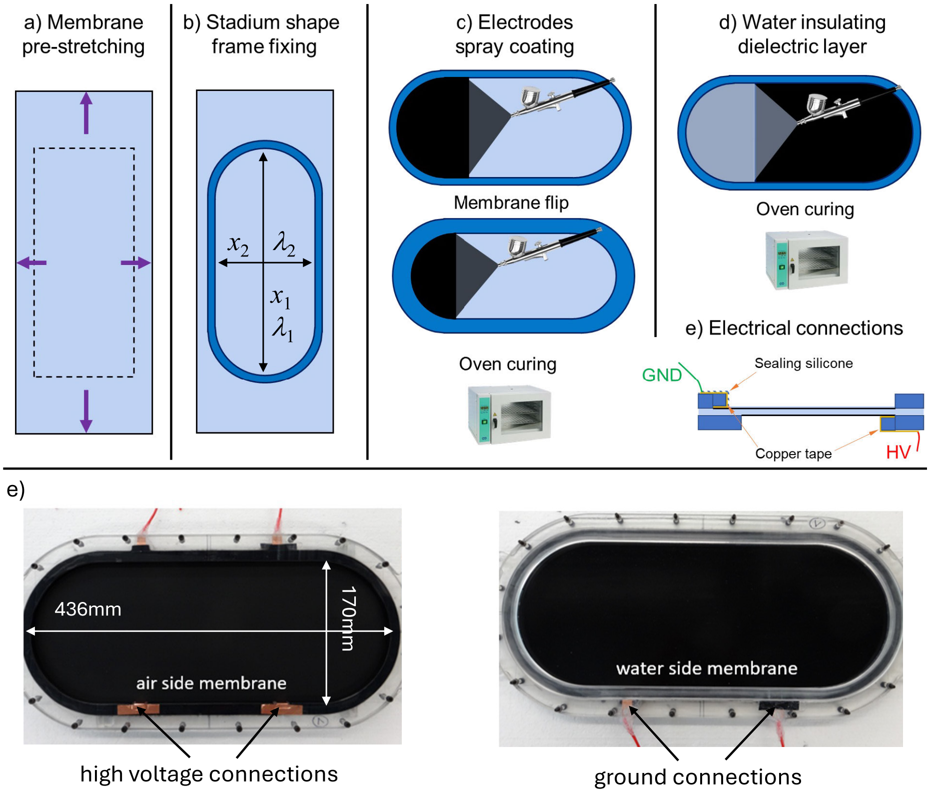

FIGURE 5. Manufacturing process of the stadium-shaped DEG: a) membrane pre-stretching; b) application and bonding of stadium shape frames; c) electrodes spraying; d) application of the insulation layer on the "water-side"; e) picture of the two sides of one of the obtained DEG membrane.

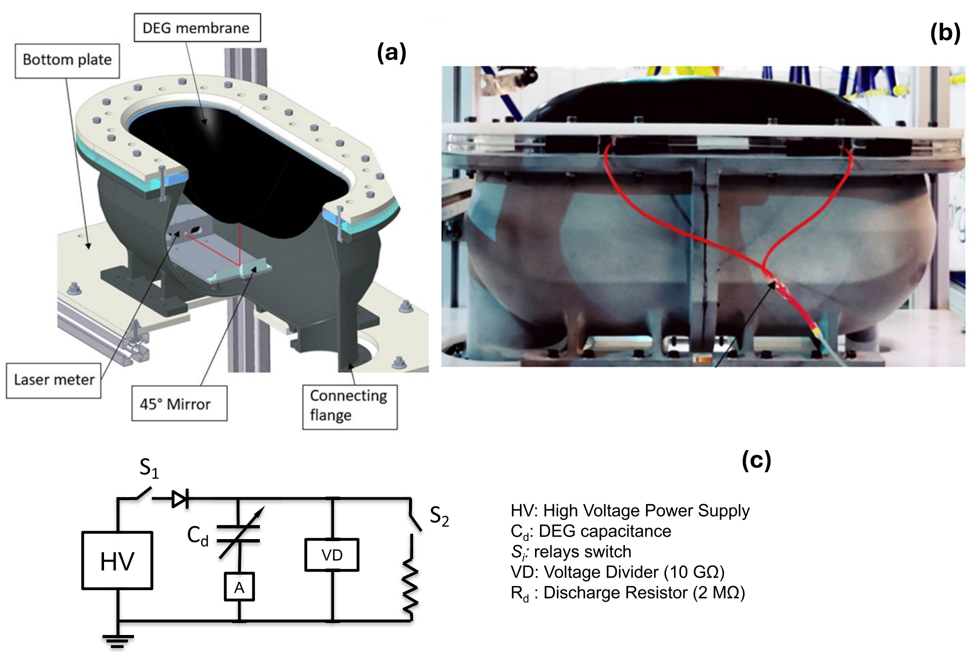

FIGURE 6. SS-PD-DEG Prototype: (a) CAD Model of the scaled SS-PD-DEG prototype showing the arrangement of the components and laser sensor for tip displacement measurement; (b) the complete experimental prototype of the SS-PD-DEG cell; (c) scheme of the driving electronics of the SS-PD-DEG employed for energy generation tests.

depressurize the system during generation tests. Additionally, the vessel hosts a laser sensor at its bottom, along with a simple optical mirror system used to divert the laser by 90°. This system is employed to measure the out-of-plane displacement of the central point of the membrane, in order to track the deformation level.

The vessel structure has been 3D-printed in Nylon 12 (PA12) using Hewlett-Packard HP Multijet Fusion 4200. The manufacturing is done in two halves due to the workspace limitations of the printer, and it is joined using an O-ring in between to guarantee sealing. All threads in the nylon structures are reinforced with metal Helicoils. A picture of the complete setup is presented in Fig. 6.

C. ELECTRONICS AND CONTROL

A dedicated electronic and control system has been developed with the following main functionalities: 1) control the inflation/deflation of the membrane; 2) drive the electrical activation/deactivation; 3) control the overall system and acquire synchronously the relevant variables.

Inflation and deflation (represented as phases P1 and P3 in Fig. 1) of the membrane is controlled with an inlet pneumatic electro-valve connected to a compressor and an outlet electro-valve that discharge toward atmospheric pressure (both valves are PNEUMAX 828.52.3.9.M2).

The electrical activation of the of the DEG membrane is implemented according to the generation cycle of Fig. 2. The electrical schematic of the employed electronics is presented Fig. 6-c. Specifically, a regulated variable high voltage power supply (ULTRAVOLT 10C24-P125-I10) is employed to set the initial priming voltage (phase P2 of Fig. 1) and a shunt resistor ($R_d = 10\text{M}\Omega$) is used for discharging (phase P4 of Fig. 1). Two reed-relays (Toward Technologies LRL-10-PCZ-20KV), S1 and S2, are employed respectively to connect the DEG to high voltage power supply and to a shunt resistor. A custom voltage divider (10 GΩ impedance, 2000:1 ratio) is used to continuously measure the high-voltage potential applied across the DEG electrodes.

The acquisition and control system is capable of acquiring differential pressure across the DEG membrane, displacement of the membrane central tip, voltage applied to the electrodes, and signals from additional monitoring sensors used to stop the system in case of flooding during underwater tests. Based on Beckhoff architecture it comprises:

- an embedded PC CX5140, operating at a 1 kHz sampling rate, for test-bench control and data acquisition;
- a differential pressure module EM3701 for continuous measurement of the pressure difference across the DEG membrane;
- a two-channel differential analogue input module EL3102 for the acquisition of:
  - the Panasonic HL-G112 laser sensor, used to continuously monitor DEG membrane tip deflection;
  - the voltage across the voltage divider;
- a first digital output terminal EL2002 controlling two electro-actuated valves;
- an analogue output terminal EL4132 driving and setting the desired voltage for the high-voltage power supply;

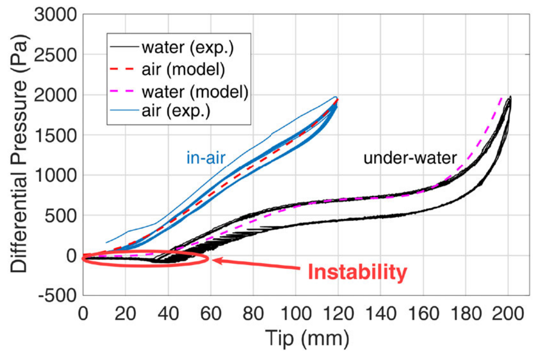

FIGURE 7. Mechanical response of the membrane, comparison between in-air and underwater. Dotted lines represented the model prediction. Red circled area represent a zone in which the membrane present a unstable/marginally stable behavior.

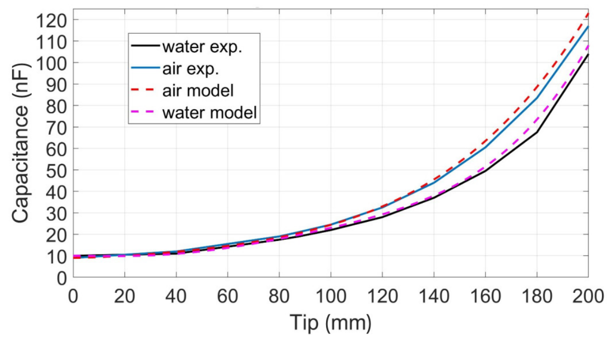

FIGURE 8. Comparison of capacitance variation against tip displacement for in-air vs underwater. Dotted lines represented the model prediction.

- a second digital output terminal EL2002 controlling two high-voltage reed relays;
- an LCR meter (R&S HM8118) employed for capacitance measurements.

V. TEST FOR MODEL VALIDATION AND DEMONSTRATION

The integrated prototype of the SS-PD-DEG described in the previous section has been tested in different conditions. Two main type of tests has been conducted: 1) model validation test that aimed at validating the electromechanical response of the system in both in-air and underwater operation; 2) generation demonstration tests in which the prototype is employed for the implementation of full generation cycles in in-air and underwater operation. The following subsections provided details of these two type of tests and the obtained results.

A. MODEL VALIDATION

Validation of the FE model has been carried out against two types of tests: 1) capacitance variation tests and 2) tip deflection at different pressure levels within the vessel. The tests were carried out on the test bench described in Section IV-B, on the assembled DEG sample (DE membrane + electrodes + protection coating layer). Validations

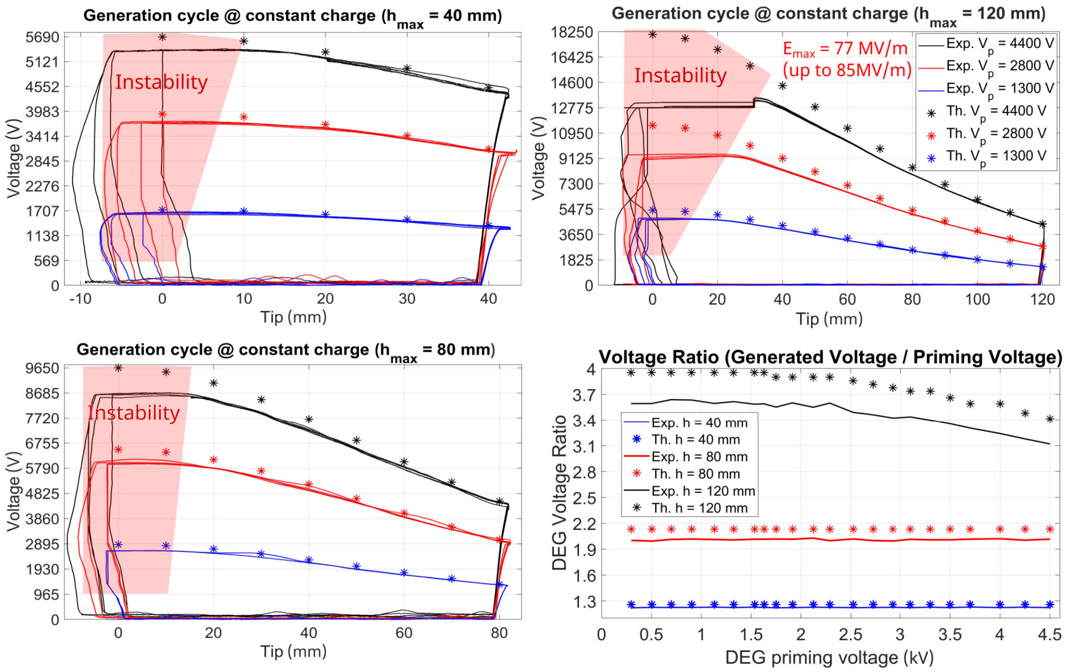

FIGURE 9. **Results for the in-air tests obtained at different priming voltages. Top-left: voltage against tip displacement for maximum tip displacement $h = 40$ mm. Bottom-left: voltage against tip displacement for maximum tip displacement $h = 80$. Top-right: voltage against tip displacement for maximum tip displacement $h = 120$. Bottom-right: obtained voltage ratio for the three level of displacement against priming voltage level.**

were carried out using the FE model implementation described in Section III-B, using the total DEG thickness (including electrodes and passive layers) for the mechanical analysis, and the dielectric thickness t_d (see Eq. (3)) for the calculation of the capacitance.

Tests were first conducted *in-air*, i.e., both sides of the membrane were in contact with air, with the external side at constant atmospheric pressure while the internal side pressure was regulated to induce out-of-plane deformation of the DEG membrane. The pressure was set in the range of $0 - 2000$ Pa. Specifically, the maximum pressure of 2000 Pa was initially applied, and a regulated leak valve was used to slowly deflate the membrane.

The same procedure was implemented for *underwater tests*. In this case, the prototype was installed underwater in a small basin shown in Fig. 11, with the membrane flange positioned at a depth of 200 mm. The membrane was initially pressurized to reach a flat position, after which a differential pressure was applied, up to a maximum of 2000 Pa. For both in-air and underwater tests, the membrane tip displacement was measured using a laser sensor, and capacitance was measured with a LCR bridge (Hameg Instruments LCR meter HM 8118).

Results of tip displacement versus pressure are presented in Fig. 7. The differential pressure corresponds to the gauge pressure measured in the air chamber and, for the case of underwater tests, it corresponds to p_a defined in Section III-B. A relatively good match can be observed between the numerical predictions obtained from the FE models. Most discrepancies are attributable to hysteresis phenomena, which were not accounted for in the developed FEM model. In-air and underwater configurations exhibit sensibly different responses. In particular, the underwater system has lower stiffness, resulting in larger displacements for a same differential pressure compared to in-air operation. This behaviour is foreseen by the models and explained by the known negative stiffness effect introduced by the displacement of the surrounding water mass. In the neighborhood of the flat position, a flat region (corresponding to quasi-zero pressure) can be observed for the underwater DEG, where the system has a marginal stable behaviour with quasi-zero stiffness.

Results of the capacitance tests are presented in Fig. 8, where the measured capacitance is plotted against the measured membrane tip displacement. It can be observed that the capacitance variation is slightly different for in-air and underwater tests, with underwater showing slightly lower capacitance values for the same displacement. This can be explained by the different shapes assumed by the membrane in the two cases. In air, the membrane is subject to uniform pressure on both sides, while when submerged, the external pressure increases with depth, and it is maximum at the membrane tip. This causes the membrane to assume a more laterally expanded geometry compared to the underwater case, which results in higher capacitance. From the figure, it can also be noted that the developed model is accurate in predicting the capacitance variation and is able to capture the different trends between in-air and underwater operation.

B. GENERATION DEMONSTRATION: IN-AIR AND UNDERWATER

In this section, the capability of the SS-PD-DEG to convert effectively inputted mechanical energy into electricity is evaluated specifically comparing the two condition of in-air and underwater operation.

In-air generation tests were carried out at constant charge, while continuously monitoring the voltage across the DEG membrane using a high-impedance voltage divider. The generation cycle, illustrated in Fig. 6, was implemented according to the following sequence:

1) Inflate the membrane to reach the desired tip displacement (with switch S2 closed);
2) Apply a pre-set priming voltage by opening S2 and then closing switch S1;
3) Open switch S1 and deflate the membrane until it returns to a flat configuration;
4) Discharge the system by closing switch S1.

Fig. 9 presents the in-air generation cycles for three different membrane tip displacements: 40 mm, 80 mm, and 120 mm. The bottom-right panel reports the corresponding voltage amplification ratios as a function of the applied priming voltage for each displacement. Theoretical predictions of the voltage-tip displacement path are included in each plot and indicated with markers. These were obtained using the measured values of the tip displacement h and the static map of the capacitance $C(h)$ shown in Fig. 8. Knowing the activation voltage V_0 used in each test (i.e., the voltage applied at maximum h_{max} to prime the DEG), the voltage in a generic deformed configuration was estimated by assuming constant charge:

$$V(h) = \frac{C_{max} V_0}{C(h)} \tag{4}$$

As observed, the discrepancies between experimental and theoretical values increase with higher activation voltages. This behavior can be primarily attributed to two factors: 1) charge leakage, which becomes more pronounced as the electric field intensifies; 2) electromechanical instabilities of the membrane occurring during the final stage of deflation, when the membrane approaches a flat configuration and the combined effect of high voltage and reduced mechanical stress may trigger local instabilities.

It is worth noting that these discrepancies are expected to contribute only marginally to the overall energy loss. They occur in a phase where the capacitance variation is minimal, due to the flatness of the capacitance–displacement curve near the flat configuration (see Fig. 8), and therefore have limited impact on the net harvested energy. This is confirmed by the relatively good value of electrical efficiency, defined as the ratio between the measured electrical output and the ideal (lossless) output corresponding to the measured capacitance variation, shown in Fig. 10-top and the energy density, defined as the ratio between the output energy and the weight of the DEG membrane, shown in Fig. 10-bottom.

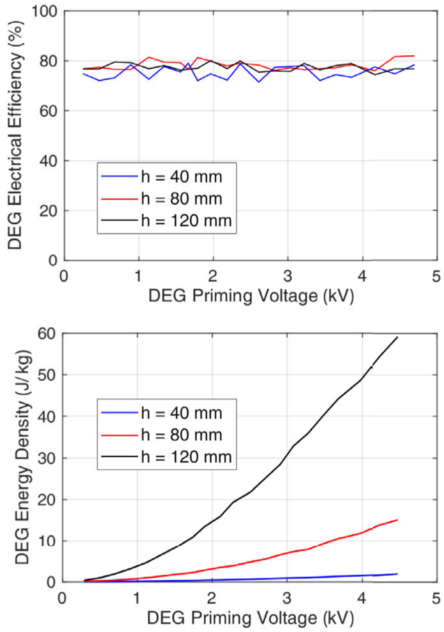

FIGURE 10. Results for in-air tests. Top: electrical efficiency, defined as the ratio between the measured electrical output and the ideal (lossless) output corresponding to the measured capacitance variation. Bottom: energy density, defined as the ratio between the output energy and the weight of the DEG membrane.

Underwater tests have been conducted in a large water pool basin. The SS-PD-DEG has been submerged 200 mm below the water level and a bias pressure has been applied to recover the flat condition compensating the hydrostatic contribution of the water column on the top of the membrane (see DEG neutral condition in Fig. 11). The generation cycle has been simulated by inflating the DEG membrane (i.e., increasing the air pressure in the vessel) with the same procedure adopted for the in-air test. However in this case a capacitance of 9 nF has been used in parallel to the DEG membrane to limit the voltage swing [9]. Test were repeated in-air and underwater in the same conditions. The energy generation results at three different excitation voltages are shown in Fig. 12. As it can be seen in the picture, there is only a slight performance reduction of under underwater tests when compared to in-air tests. These tests were reliable up to very large tip deflection of up to 120 mm, corresponding to a pressure variation of approximately 700 Pa (see Fig. 7) in the air chamber .

As highlighted in red in Fig. 12 and 7, the underwater voltage lines change slope in the last part of the voltage increase phase (Fig. 2) and the pressure lines become flat. This is due to the negative stiffness contribution introduced by the hydrostatic head above the membrane. In this region, the variation of the potential elastic energy of the membrane is balanced by the variation of the gravitational potential energy of the hydrostatic head above the membrane. This energy compensation allows the cell to operate in a wide range of wave frequencies as mentioned in Section I.

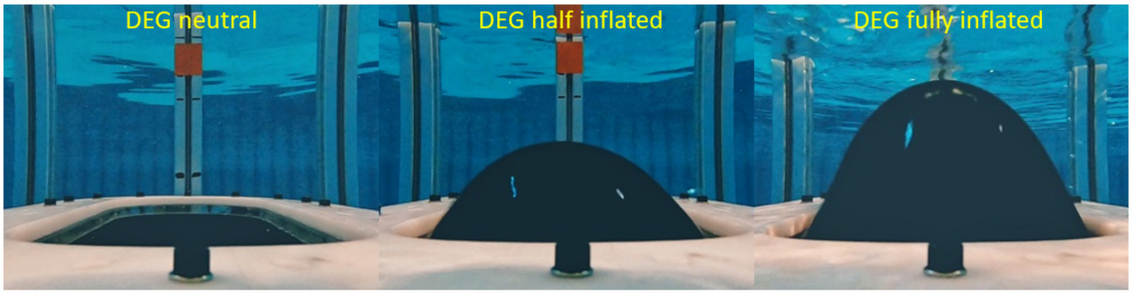

FIGURE 11. Pictures of the SS-PS-DEG during underwater test showing three levels of inflation of the membrane.

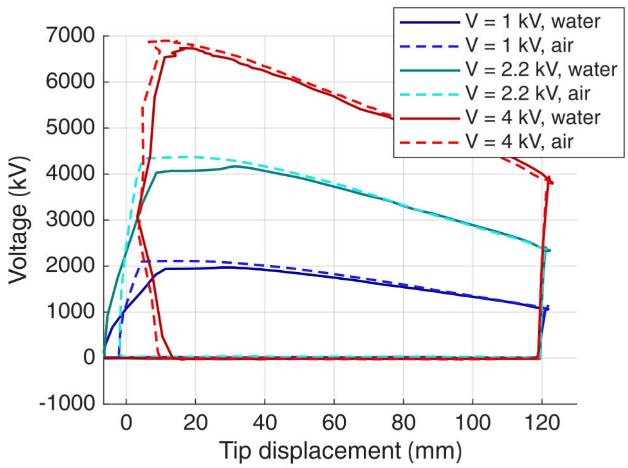

FIGURE 12. Electricity generation cycles, in-air and underwater. Experimental voltage lines for three different excitation voltages.

C. DISCUSSION

The experimental results obtained in underwater tests provide estimates of the performance of small scale SS-PD-DEGs operating in a WEC. Accurately predicting WEC performance in realistic dynamic working conditions is a complex task that demands accounting for multiple dynamic contributions such as inertial loads, friction forces, and hydrodynamic loads. Dynamic models of pressure differential WECs based on circular submerged DEGs have been developed and validated in previous works [13].

The tests performed in the present study are representative of the quasi-static performance of a small-scale SS-PD-DEG. Nonetheless, they can be used to obtain a rough estimation of the performance of a full-scale WEC housing an up-scaled version of the DEG, as done by previous works on DEGs [10].

In particular, a projection using a scale-up factor has been conducted under the following assumptions/simplifications:

1) Quasi-static response: The mechanical and electrical behavior of the membrane is assumed to remain quasi-static (i.e. independent of period/frequency) during the wave cycle. Dynamic effects such as inertial and viscous damping are neglected, based on the relatively low oscillation frequencies (order of 0.1–0.2 Hz) typical of ocean waves. Under this assumption a nominal wave period of 7 s is adopted as representative of a sea state of moderate intensity in the target operating environment (such as EMEC wave test site [21]). This allows estimating the average electrical power output from the energy converted per cycle under regular wave excitation.
2) Froude-consistent scaling laws: The performance extrapolation follows previously validated Froude-scaling relationships for DEG-based PTO systems [13], [22]. Accordingly, the DEG tip displacement and equilibrium pressure scale linearly with the geometric factor, provided that the active dielectric volume scales with the fourth power of the scale factor—meaning the membrane thickness increases with the square of the scale factor. Under these conditions, the converted energy density remains invariant.
3) Point-absorber assumption still holds: The up-scaled WEC is assumed to maintain the point-absorber configuration. Even when scaled up, the device's characteristic dimensions (e.g., a minor axis of approximately 5 m for a 30× scale-up) remain significantly smaller than typical ocean wavelengths [23], ensuring that the SS-PD-DEG experiences nearly uniform wave pressure across its surface.
4) Energy density: The energy density data obtained from in-air tests at 4.5 kV are assumed to approximate those achievable underwater, given the comparable capacitance–displacement trends observed in both conditions (see Fig. 8). This simplification enables the use of in-air experimental data to estimate underwater energy conversion performance.

The obtained results are shown in Fig. 13, which illustrates that the DEG could provide power outputs within the broad range of 10-100 kW with wave heights of 1-2 m and scale factors of 5-40 times. The red shaded area in the figure denotes configurations in which the DEG tip displacement would exceed the conservative limit used in the tests (h = 120 mm at the scale of our setup). To operate in those

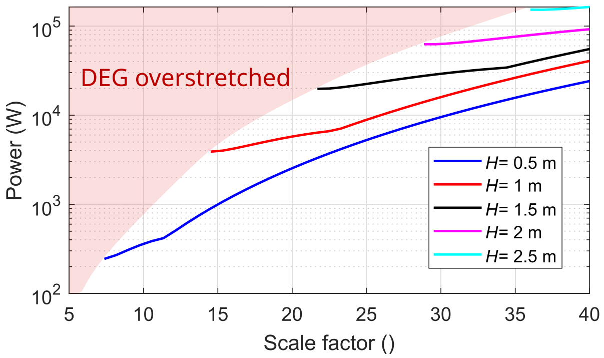

FIGURE 13. Projection of the power generated by a full-scale SS-PD-DEG as a function of the scale factor, for incident waves with a period of 7 s and different wave heights. These estimates are based on experimental quasi-static results shown in Fig. 10.

area the DEG would require protection mechanisms such as chamber pre-pressurization regulation [13]) or mechanical restraints.

While these numbers represent rough orders of magnitude, they suggest that up-scaled versions of the presented SS-PD-DEG could allow hitting power values compatible with the targets of large scale energy harvesting. It is worth remarking that the tests presented here (and, hence, the obtained estimates for the convertible energy density) refer to relatively low values of the maximum applied electric field (on the order of 70 kV/mm at the maximum DEG deformation), and to sub-optimal constant-charge control cycles. These power values could be drastically increased by resorting to higher electric field, compatible with the material limits [24], [25], and more advanced controls (e.g., constant voltage or constant electric field cycles [8]). Overall, these figures of merit prove that a significant margin of improvements exists.

VI. CONCLUSION

This paper presents the design, modelling, fabrication, and testing of a stadium-shaped Dielectric Elastomer Generator (SS-PD-DEG), which is a candidate power take off (PTO) system for pressure differential submerged wave energy converters. A dedicated finite element model was developed and validated against experimental results to capture the complex non-axisymmetric deformation of the stadium-shaped membrane and to predict its capacitance variations under both uniform and hydrostatic pressure loading.

A small-scale generator prototype was fabricated and tested in both in-air and submerged conditions. The experimental results confirmed the capability of the proposed system to perform complete energy generation cycles while directly operating in conductive environments. In-air and underwater measurements were in good agreement with theoretical predictions, with observed discrepancies at high voltages attributed to charge leakage and membrane instabilities near the flat configuration. Importantly, these discrepancies were shown to have only a limited impact on net energy harvesting, as they occur in regions of minimal capacitance variation. A small-scale generator prototype was fabricated and tested both in-air and submerged conditions. The experimental results confirmed the capability of the proposed system to perform complete energy generation cycles while directly operating in conductive environments. In-air and underwater measurements were in good agreement with theoretical predictions, with observed discrepancies at high voltages attributed to charge leakage and membrane instabilities near the flat configuration. Importantly, these discrepancies were shown to have only a limited impact on net energy harvesting, as they occur in regions of minimal capacitance variation.

The underwater experiments demonstrated that the SS-PD-DEG can operate reliably in direct contact with water, with performance comparable to in-air tests. The negative-stiffness effect induced by hydrostatic loading was experimentally observed and confirmed to provide extended deformability and potential for broadband frequency response, a critical feature for efficient wave energy harvesting.

Overall, this work provides one of the first experimental proofs of submerged DEG-based PTOs in active operation. The results highlight the potential of SS-PD-DEGs to reduce complexity and costs compared to conventional pneumatic PTOs, while offering silent, corrosion-resistant, and scalable solutions for wave energy conversion. Future studies will aim to validate these findings under controlled wave-tank conditions, where both regular and irregular wave fields can be reproduced to investigate the dynamic coupling between the SS-PD-DEG, the hydrodynamic loads, and the electrical control strategies. Such experiments will be important to confirm and refine the scaling projections presented in this work, define the wave-to-wire performance models, and thus strengthen applicability of SS-PD-DEG technology in realistic offshore energy harvesting scenarios. Additionally, future work will address long-term stability in marine environments, optimizing large-scale modular arrays, and integrating tailored electrical drives to preserve efficiency at the device and system level.

ACKNOWLEDGMENT

The authors would like to thank Francesco Damiani, Electronic Technician at Scuola Superiore Sant'Anna, for his technical support during the prototype design and testing. Views and opinions expressed are those of the authors only and do not necessarily reflect those of the European Union or the European Research Council. Neither the European Union nor the granting authorities can be held responsible for them.

REFERENCES

[1] K. Gunn and C. Stock-Williams, "Quantifying the global wave power resource," *Renew. Energy*, vol. 44, pp. 296–304, Aug. 2012.

[2] C. Kalogeri, G. Galanis, C. Spyrou, D. Diamantis, F. Baladima, M. Koukoula, and G. Kallos, "Assessing the European offshore wind and wave energy resource for combined exploitation," *Renew. Energy*, vol. 101, pp. 244–264, Feb. 2017.
[3] A. Cornett, "A global wave energy resource assessment," in *Proc. ISOPE Int. Ocean Polar Eng. Conf.*, May 2008, pp. 1–9, Paper ISOPE-2008-TPC-579.
[4] A. Pecher and J. P. Kofoed, *Handbook of Ocean Wave Energy*. Cham, Switzerland: Springer, 2017.
[5] A. F. D. O. Falcão, "Wave energy utilization: A review of the technologies," *Renew. Sustain. Energy Rev.*, vol. 14, no. 3, pp. 899–918, Apr. 2010.
[6] G. Moretti, M. Santos Herran, D. Forehand, M. Alves, H. Jeffrey, R. Vertechy, and M. Fontana, "Advances in the development of dielectric elastomer generators for wave energy conversion," *Renew. Sustain. Energy Rev.*, vol. 117, Jan. 2020, Art. no. 109430.
[7] M. Liu, R. J. Young, and L. Chen, "Next-generation wave energy harvesting with dielectric elastomer generators," *IEEE Elect. Insul. Mag.*, vol. 41, no. 2, pp. 15–23, Mar. 2025.
[8] G. Moretti, S. Rosset, R. Vertechy, I. Anderson, and M. Fontana, "A review of dielectric elastomer generator systems," *Adv. Intell. Syst.*, vol. 2, no. 10, Oct. 2020, Art. no. 2000125.
[9] S. Shian, J. Huang, S. Zhu, and D. R. Clarke, "Optimizing the electrical energy conversion cycle of dielectric elastomer generators," *Adv. Mater.*, vol. 26, no. 38, pp. 6617–6621, Oct. 2014.
[10] R. Kaltseis, C. Keplinger, S. J. Adrian Koh, R. Baumgartner, Y. F. Goh, W. H. Ng, A. Kogler, A. Tröls, C. C. Foo, Z. Suo, and S. Bauer, "Natural rubber for sustainable high-power electrical energy generation," *RSC Adv.*, vol. 4, no. 53, pp. 27905–27913, 2014.
[11] G. Moretti, A. Scialò, G. Malara, G. G. Muscolo, F. Arena, R. Vertechy, and M. Fontana, "Hardware-in-the-loop simulation of wave energy converters based on dielectric elastomer generators," *Meccanica*, vol. 56, no. 5, pp. 1223–1237, May 2021.
[12] G. Moretti, G. Malara, A. Scialò, L. Daniele, A. Romolo, R. Vertechy, M. Fontana, and F. Arena, "Modelling and field testing of a breakwater-integrated U-OWC wave energy converter with dielectric elastomer generator," *Renew. Energy*, vol. 146, pp. 628–642, Feb. 2020.
[13] M. Righi, G. Moretti, D. Forehand, L. Agostini, R. Vertechy, and M. Fontana, "A broadbanded pressure differential wave energy converter based on dielectric elastomer generators," *Nonlinear Dyn.*, vol. 105, no. 4, pp. 2861–2876, Sep. 2021.
[14] E. Taine, A. Claverie, F. Caillé, S. Shili, N. Fourdilis, J. Hendrikse, and R. Boulard, "The S3 wave energy converter story," *Proc. SPIE*, vol. 13431, p. 78, May 2025.
[15] D. M. Turner, "An S-shaped diaphragm and an energy conversion device," WO Patent 2 009 138 740 A2, May 13, 2009.
[16] S. Grey, "Module for an energy conversion device," GB Patent 2 519 282 A, Aug. 8, 2013.
[17] R. W. Ogden, G. Saccomandi, and I. Sgura, "Fitting hyperelastic models to experimental data," *Comput. Mech.*, vol. 34, no. 6, pp. 484–502, Nov. 2004.
[18] Y. Chen, L. Agostini, G. Moretti, M. Fontana, and R. Vertechy, "Dielectric elastomer materials for large-strain actuation and energy harvesting: A comparison between styrenic rubber, natural rubber and acrylic elastomer," *Smart Mater. Struct.*, vol. 28, no. 11, Nov. 2019, Art. no. 114001.
[19] G. Rizzello, P. Loew, L. Agostini, M. Fontana, and S. Seelecke, "A lumped parameter model for strip-shaped dielectric elastomer membrane transducers with arbitrary aspect ratio," *Smart Mater. Struct.*, vol. 29, no. 11, Nov. 2020, Art. no. 115030.
[20] O. H. Yeoh, "Characterization of elastic properties of carbon-black-filled rubber vulcanizates," *Rubber Chem. Technol.*, vol. 63, no. 5, pp. 792–805, Nov. 1990.
[21] L. O'Boyle, K. Doherty, J. V. Hoff, and J. Skelton, "The value of full scale prototype data-testing oyster 800 at EMEC, orkney," in *Proc. 11th Eur. Wave Tidal Energy Conf. (EWTEC)*, Sep. 2015.
[22] G. Moretti, G. P. Rosati Papini, L. Daniele, D. Forehand, D. Ingram, R. Vertechy, and M. Fontana, "Modelling and testing of a wave energy converter based on dielectric elastomer generators," *Proc. Roy. Soc. A, Math., Phys. Eng. Sci.*, vol. 475, no. 2222, Feb. 2019, Art. no. 20180566.
[23] M. E. McCormick, *Ocean Wave Energy Conversion*. Mineola, NY, USA: Dover, 2013.
[24] F. Förster-Zügel, S. Solano-Arana, F. Klug, and H. F. Schlaak, "Dielectric breakdown strength measurements with silicone-based single-layer dielectric elastomer transducers," *Smart Mater. Struct.*, vol. 28, no. 7, Jul. 2019, Art. no. 075042.
[25] E. Taine, T. Andritsch, I. A. Saeedi, and P. H. F. Morshuis, "Size effect and electrical ageing of PDMS dielectric elastomer with competing failure modes," *Smart Mater. Struct.*, vol. 32, no. 10, Oct. 2023, Art. no. 105021.

MARCO CASELLI is currently pursuing the Ph.D. degree with the Department of Industrial Engineering (DIN), University of Bologna. His expertise spans mechatronics, robotics, electroadhesive devices, and dielectric elastomer sensors. His research interests include contributions to conference papers on dielectric elastomer generators, and a multidirectional hemispherical dielectric elastomer proximity sensor for collision avoidance in human–robot interaction.

AMEDEO CARLONI is currently pursuing the Ph.D. degree with the Department of Industrial Engineering, University of Bologna, Italy. He is a Research Fellow with the Department of Industrial Engineering, University of Bologna. He has authored several publications, such as on compliant soft grippers using electro-adhesion, dielectric elastomer generators, and resonance-based mechanisms to reduce motor torque requirements. His research interest includes the development of thin-film polymer transducers for mechatronics, aimed at supporting the green transition.

ANTONELLO CHERUBINI received the degree in mechanical engineering from Politecnico di Milano and the Ph.D. degree (Hons.) in robotics from Scuola Superiore Sant'Anna, Pisa, in 2017. He is currently an Assistant Professor (RTDA) with the Department of Industrial Engineering, University of Trento, Italy. His research interests include autonomous driving, predictive safety models, electroactive transducers, and elastic actuation for energy-efficient robotics. He received the Bernardo Nobile Award.

GIACOMO MORETTI received the Ph.D. degree from Scuola Superiore Sant'Anna, Pisa, in 2017. He was a Post-Doctoral Researcher with Scuola Superiore Sant'Anna, from 2017 to 2020. He is currently an Associate Professor of mechanics of machines with the Department of Industrial Engineering, University of Trento, Italy. His research interests include smart transducers, multifunctional materials, energy harvesting, and dielectric elastomer technologies with applications spanning soft robotics, underwater systems, and acoustic devices. He was a Marie Skłodowska-Curie Fellow with the Intelligent Material Systems Laboratory of Saarland University, Germany, from 2020 to 2022. In 2024, he was awarded a European Research Council (ERC) Starting Grant for his research on electrostatic transducers.

MARCO FONTANA received the M.S. degree in mechanical engineering from the University of Pisa, Italy, in 2003, and the Ph.D. degree in innovative technologies from Scuola Superiore Sant'Anna (SSSA), Pisa, in 2008.

He is currently a Professor of mechanical engineering with the Institute of Mechanical Intelligence, SSSA, where he leads the Robotic Mechanisms and Materials Group. He has authored more than 100 publications and nine patents. His research focuses on innovative electro-mechanical solutions for robotics and energy conversion. He has been the coordinator of several research initiatives at the National and European level. His research interests include wearable and soft robotics, haptics, wave energy conversion, artificial muscles, electroactive polymers (EAP), and electrostatic transducers.

ROCCO VERTECHY received the degree in mechanical engineering, in 2001, and the Ph.D. degree in mechanics of machines, in 2005. He is currently a Full Professor with the Department of Industrial Engineering, University of Bologna, where he leads research on advanced robotics and electrostatic devices for industrial applications. He is the coordinator of the SAIMA laboratory and has authored over 100 publications and holds an international patent owned by European Space Agency. His work focuses on mechatronic systems built with smart materials and compliant mechanisms, covering both precision robotics (e.g., robotic exoskeletons, snake robots) and energy harvesting from waves and airborne wind.